Soil organic carbon enrichment triggers *in-situ* nitrogen interception by phototrophic biofilms at soil-water interface: from regional to micro scales

Junzhuo Liu[1,2*], Yanmin Zhou[1,2], Pengfei Sun[1,2], Yonghong Wu[1,2*], Jan Dolfing[3]

[1] State Key Laboratory of Soil and Sustainable Agriculture, Institute of Soil Science, Chinese Academy of Sciences, 71 East Beijing Road, Nanjing, 210008, China

[2] Zigui Three Gorges Reservoir Ecosystem, Observation and Research Station of Ministry of Water Resources of the People's Republic of China, Yichang, 443605, China

[3] Faculty of Energy and Environment, Northumbria University, Newcastle upon Tyne NE1 8QH, UK

***Corresponding author**:

Junzhuo Liu, Address: 71 East Beijing Road, Nanjing, 210008, China

Tel.: +86 25 86881308, Fax: +86 25 8688 1000; E−mail: jzhliu@issas.ac.cn

Yonghong Wu, Address: 71 East Beijing Road, Nanjing, 210008, China

Tel.: +86 25 86881330, Fax: +86 25 8688 1000; E−mail: yhwu@issas.ac.cn

18 **Graphical abstract**

19

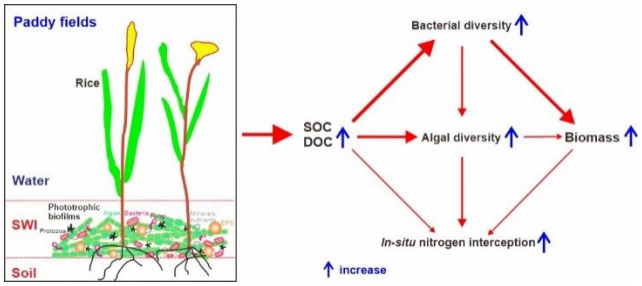

Abstract

Phototrophic biofilms are easy to grow at sediment/soil-water interfaces (SWI) in shallow aquatic ecosystems and greatly impact nutrient biogeochemical cycles. However, the pathways by which they contribute to nitrogen interception and interact with sediment/soil remains largely unknown. Here, we conducted a field investigation in paddy fields in various regions of China and found that nitrogen immobilized in biofilm biomass significantly positively correlated with soil organic carbon (SOC) content. A microcosm experiment showed that this was due to increased bacterial and algal diversity, biomass accumulation and inorganic nitrogen assimilation at high SOC especially high dissolved organic carbon (DOC) levels. The metatranscriptomics results further verified that many KO groups of PSII, PSI, AP and PC in antenna proteins and Glutamate synthesis were distinctly expressed at elevated SOC and DOC levels. Our results elucidated the effects and possible pathways of how SOC enrichment triggers photosynthesis and nitrogen immobilization by phototrophic biofilms. The results will provide meaningful information for *in-situ* nitrogen interception by using phototrophic biofilms at SWI in human-made wetlands to change internal nitrogen cycling.

Keywords: DOC, Diversity, Nitrogen interception, Metatranscriptomics, Wetland

Synopsis: A national field investigation and a microcosm experiment together elucidated that elevated soil organic carbon levels enhanced *in-situ* nitrogen interception by phototrophic biofilms at soil-water interface.

Introduction

Nitrogen discharge from agro-ecosystems has been a main contributor to surface water pollution, especially under the increasing food demand and overfertilization conditions in developing countries.[1-3] Interception of excessive nitrogen in cropland has long been challenging.[4, 5] In paddy fields, the soil-water interfaces (SWI) form the boundary between soil and water, and are the sites where the various nutrient cycles are coupled.[6, 7] As a seasonal human-made wetland, the periodic alternation of wetting and drying and fertilization in paddy fields initiates and drives formation and withering of phototrophic biofilms at SWI.[8] Mainly composed of algae, bacteria and abiotic substances, phototrophic biofilms (also called periphyton[9]) form at SWI and flourish during the tilling and shooting stages (about 1.5-3 months) of rice cultivation.[1, 4, 8] By assimilating inorganic nitrogen, phototrophic biofilms immobilize nitrogen in biomass and effectively intercept *in-situ* nitrogen.[1]

Studies have reported that phototrophic biofilms can accumulate up to 70 mg N/g biomass,[10] and that this nitrogen can be released into the sediment/soil in inorganic forms when biomass gets mineralized.[8] Reynaud and Roger [11] reported that in one growth season, algal biomass accumulated in one ha of paddy fields ranged between several hundred kg to more than one ton. Thus, in one ha paddy fields, phototrophic biofilms may immobilize dozens of kilograms of nitrogen. In many places farmers build ecological ditches or buffer strips to trap and filter nutrients from runoff.[12] Hence, even though the paddy phototrophic biofilms may get washed away during heavy rains, nitrogen immobilized in biofilm biomass is easier to intercept by ecological ditches than nitrogen dissolved in water. Moreover, drainage and drying in paddy fields can prompt the withering and decay of phototrophic biofilms[1], with consequent nitrogen release into soil to supply to rice plants. However, the contribution of phototrophic biofilms to *in-situ* nitrogen interception in paddy fields has been largely overlooked in the past.[1]

Function and functionality of a community depend largely on its composition, and due to complementarity effects, especially on its diversity.[13-15] Assimilation is the main pathway of inorganic nitrogen immobilization by phototrophic biofilms, however, both algae and bacteria have phylogenetic differences in nitrogen uptake capacity for different forms of nitrogen.[16, 17] In soil, nitrogen exists in various forms and species-rich communities have advantages in immobilizing different forms of nitrogen.[15, 18]

Given the continuously changing physiochemical conditions at SWI, the community structure and metabolic activities of phototrophic biofilms may vary greatly, resulting in changes in biofilm growth and nitrogen immobilization capacity.[19] However, current studies on phototrophic biofilms mainly focus on their applications in nutrient removal from wastewater, where they grow on artificial substrates and carbon and nutrient exchanges with soil are absent.[20-22] Hence, the effects of soil physiochemical conditions on the community structure and photosynthesis of phototrophic biofilm, and its contribution to nitrogen interception in paddy fields deserve further studies.

In paddy fields, soil organic carbon (SOC), affects soil texture, water content and pH, and provides essential substrate and nutrients for phototrophic biofilms.[23-25] Formation of phototrophic biofilms starts with colonization by heterotrophic bacteria and the production of adhesive extracellular polymeric substances (EPS) as a matrix on solid surfaces, subsequently followed by the immigration and adhesion of algae.[22, 26, 27] During this process, sufficient SOC supply facilitates the colonization of various bacterial species and secretion of polysaccharides, which help different algal cells to adhere to the biofilm matrix and help stabilize the biofilm community with high diversity.[27, 28] Via this pathway nitrogen immobilization capacity of phototrophic biofilms gets influenced, but the driving effects and underlying mechanisms of SOC still remain largely unknown.[10, 22] In the complex mixture of components that SOC is, dissolved organic carbon (DOC) such as humic acids, proteins, vitamins and amino acids is the most labile and active fraction with potent effects on the growth of algae and bacteria.[29, 30] To make full use of phototrophic biofilms for *in-situ* nitrogen retention in paddy soils, the effects of SOC and DOC deserve intensive study, especially in China, where nitrogen is excessively used in paddy fields and retention is paramount.[31] High-throughput sequencing technologies such as the full-length 16S and 18S rRNA gene amplicon sequencing and metatranscriptomics should enable to precisely identify the functioning species and reveal the potential activities of complex microbial communities and the underlying mechanisms that regulate them in phototrophic biofilms grown under varying SOC conditions in paddy fields.[32, 33]

In this study, we conducted a large-scale field investigation and microcosm experiments to elucidate the effects of SOC on the community characteristics and nitrogen immobilization functions of phototrophic biofilms and the underlying

mechanisms. Our research hypothesis was that SOC affects both the community structure and the nitrogen immobilization functions of paddy phototrophic biofilms. We addressed the following three questions: (1) How do the community structure and nitrogen immobilization capacity of phototrophic biofilms vary along SOC gradients? (2) What are the effects of community structure of paddy phototrophic biofilms on nitrogen immobilization? (3) What is the underlying mechanism of the influence of SOC on nitrogen interception by phototrophic biofilms at SWI?

Materials and methods

Collection and analysis of paddy phototrophic biofilms

To obtain a general relationship between SOC and phototrophic biofilm functions in paddy fields, 20 sites in three of the six main rice planting regions in China[34] were selected (Fig. S1). They were South China (region I), the middle and lower reaches of Yangtze River (region II), and Northeast China (region III). Paddy phototrophic biofilms were collected during May to July in 2016 and 2017, depending on the rice transplanting time in the different regions. Samples were collected about 20 days after rice transplanting, at which time the plants were in tillering stage and phototrophic biofilms were thick. Specifically, about 200 g biofilm biomass (wet weight) was peeled off from the submerged soil surface with tweezers and razor knives. Meanwhile, after having first scraped off and removed the attaching phototrophic biofilms from soil, individual samples of about 500 g surface soil (top 0-5 cm) were collected with a shovel. At each site, ten samples were collected from ten rice planting parcels within an area of 10 km^2. After being transported to the laboratory preserved on ice, paddy phototrophic biofilms samples were stored at -20°C and then freeze-dried to measure their nitrogen contents. Soil samples were air-dried under indoor conditions and then crushed and passed through 0.15 mm sieves to measure their contents of soil total organic carbon (SOC) and soil total nitrogen (STN).

Microcosm experiment under varying SOC conditions

To elucidate the mechanism as to how SOC influences the growth and nitrogen accumulation of phototrophic biofilms, a microcosm experiment was conducted. Specifically, surface soil (0-30 cm) collected from a paddy field in Jurong, Jiangsu

Province, China was air-dried, crushed and passed through 1 mm sieve for a pot experiment. The characteristics of the paddy soil were as follows: pH 5.8±0.1, SOC 2.32±0.2%, total nitrogen (TN) 1.72±0.12 g/kg, total phosphorus (TP) 0.42±0.04 g/kg, and DOC 272.2±3.4 mg/kg. To obtain a gradient of SOC content, 80 g paddy soil was mixed with 0.4 g, 0.8 g, 1.2 g, 1.6 g, 2.0 g and 2.4 g fermented and crushed peanut shell (organic carbon content of 41%, piece size of 1-2 mm) respectively, designated as treatments A, B, C, D, E and F. A paddy soil without adding peanut shell was set as control (CK); all the treatments were set up in triplicates. The mixture of soil and peanut shell was placed in crystallizing dishes (diameter 90 mm). To provide sufficient nutrient and mimic fertilizer application in paddy fields, $NaNO_3$ and KH_2PO_4 were diluted in distilled water at concentrations of 2.8 NO_3^--N mg/L and 0.15 PO_4^{3-}-P mg/L respectively, and in each dish 140 ml of the abovementioned medium was added, resulting in a water layer of 1 cm. To prevent atmospheric deposition, the crystallizing dishes were covered with sealing film with holes for aeration. The microcosm experiment was conducted in a greenhouse in Nanjing, China, and lasted for 30 days during May to July 2020 with temperatures of 18-30°C. To compensate for evaporation, every two days distilled water was added to dishes to keep a water layer of 1 cm.

On day 2, soil samples were collected from each dish to measure SOC and DOC. On day 30, dense phototrophic biofilms had formed at SWI and were collected for analysis. The wet biomass of phototrophic biofilms was first weighed and then part of it was quick-frozen with liquid nitrogen and preserved at -80°C for full-length 16S and 18S rRNA sequencing and metatranscriptomic analysis. Part of the wet biomass was used to measure EPS contents. The rest of the biomass was freeze-dried to measure the water content and total nitrogen content.

Chemical analyses

SOC and STN contents of soil samples were analyzed using a C/N analyzer (FLASH 2000 NC Analyzer, Thermo Scientific) after removing carbonate in soil by adding 0.1 M HCl. DOC was measured using a TOC analyzer (LCPH, Shimadzu, Japan) after an extraction of 2.5 g dry soil in 15 ml ultra-pure water. Dry weight (biomass) of phototrophic biofilms from the microcosm experiment was obtained by multiplying the wet weight by the moisture content. Nitrogen content of phototrophic biofilm biomass (biomass N) collected from both paddy field and the microcosm experiment was

166 measured using an ICP-OES (ICPOES730, Agilent, U.S.A) by using 20 mg freeze-
167 dried biomass per sample. EPS of phototrophic biofilms was extracted from 200 mg
168 wet biomass using NaOH and polysaccharide and protein contents were determined by
169 anthrone-H_2SO_4 colorimetry and the bicinchoninic acid (BCA) method, respectively[35]
170 and expressed as mg/g dry biomass by multiplying with the moisture content of each
171 phototrophic biofilm sample.

172 *16S and 18S rRNA amplicon analysis*

173 To determine the community composition of phototrophic biofilms of the
174 microcosm experiment, DNA was extracted from wet biomass using the CTAB/SDS
175 method.[36] The primers 27F (AGRGTTYGATYMTGGCTCAG) & 1492R
176 (RGYTACCTTGTTACGACTT) and Euk-A (AACCTGGTTGATCCTGCCAGT) &
177 Euk-B (GATCCTTCTGCAGGTTCACCTAC) were used for PCR amplification of
178 full-length 16S rRNA and 18S rRNA genes respectively.[37] The PCR reactions were
179 carried out with TransStart® FastPfu DNA Polymerase (TransGen Biotech, Beijing,
180 China). Electrophoresis on 2% agarose gel was performed to detect and remove
181 undesired PCR products. The gels were then extracted with QIAquick Gel Extraction
182 Kit (Qiagen, Venlo, NL) and purified with AMPure PB beads (PacBio, CA,
183 USA). Sequencing libraries were generated using the SMRTbell™ Template Prep Kit
184 (PacBio). Sequencing was performed on the PacBio Sequel platform at Novogene
185 (Tianjin, China). After sequencing, raw sequences were first processed through the
186 PacBio SMRT portal and aligned to each other to generate circular consensus sequences.
187 Then the files were used for amplicon size trimming and sequences smaller than 1340
188 bp or larger than 1640 bp were removed. The reads were compared with the reference
189 database using UCHIME Algorithm to detect and remove chimera sequences.
190 Operational Taxonomic Unit (OTU) classification was performed with a 97% identity
191 cut off using Uparse v7.0.1001. The SSU rRNA Database of Silva Database was used
192 to annotate taxonomic information. In this study, the taxonomic structure compositions
193 of algae and bacteria in phototrophic biofilms were selected to calculate the relative
194 abundance of different groups at each classification level.

195 *Metatranscriptomics analysis*

196 The total RNA was extracted using PowerSoil™ Total RNA Isolation Kit (MoBio)

with RNA quantity and quality assessed with the Bioanalyzer 2100 (Agilent). RNA libraries were prepared as rRNA depletion and stranded method. The ribosomal RNA was firstly depleted from total RNA using the rRNA Removal Kit and then fragmented into 250-300 bp fragments and reverse-transcribed into cDNA. The cDNA fragments were amplified using PCR. Then, the library concentration was measured by the Qubit® fluorometer and adjusted to 1 ng/μL. After building the library and pooling of different samples, samples were sequenced on Illumina (PE150) at Novogene Co., LTD. Thereafter, raw reads were processed through in-house perl scripts to get clean reads by removing the poor quality-based and adapter sequences. After that, de novo assembly was performed on the clean reads with Trinity and sequences of all samples were integrated and repeat was deleted using CH-HIT-EST to obtain unigene dataset.

In order to obtain comprehensive gene function information, the database KEGG was used for gene function annotations. To quantify the differential expression of genes, the clean reads of each sample were mapped to reference sequence which was spliced by Trinity. Quantification of the transcripts and genes was performed with the Fragments Per Kilobase of transcript sequence per Millions base pairs (FPKM)-normalization method using RSEM. DESeq2 was used for differential expression analysis and the resulting p values were adjusted using Hochberg's approach and genes with $|\log2\ (\text{Fold Change})| > 0$ & $p_{adj} < 0.05$ were assigned as differentially expressed. Moreover, the differentially expressed genes were aligned to the KEGG Pathway Database to identify the enriched pathways, using the hypergeometric distribution model. Then, the proportion of differentially expressed genes mapping to each KO group relative to all KEGG annotated genes at that KO group was calculated, referring to as rich factor.

Statistical analysis

Box plots were employed to show the SOC and biomass nitrogen contents in phototrophic biofilms collected from the 20 sampling sites in China. One-way ANOVA was used to test the differences in SOC, DOC, biomass, biomass N and EPS contents among different treatments by applying a significance level of 0.05 with SPSS 22.0. Using the OTUs, the community diversity of algae and bacteria were separately evaluated by Shannon-Wiener index using the package 'vegan' in R.[38] To evaluate the

correlations between SOC, DOC, and phototrophic biofilm biomass, nitrogen immobilization capacity, diversity and community composition, Spearman correlation analyses for pairwise complete data were performed using package 'psych' in R, and a correlation heatmap was used to visualize the results using package 'pheatmap' in R.[39] To elucidate the effects of SOC and DOC on biomass accumulation and nitrogen immobilization in phototrophic biofilms, a structural equation model (SEM) was set up. Models with different structures were evaluated using χ^2, p value, and RMSEA. SEM was conducted using the package 'lavaan' in R.[40]

Data deposition

Data sets of the phototrophic biofilm amplicon and metatranscriptomics sequences of the microcosm experiment are available through NCBI BioProject accessions PRJNA693353 and PRJNA693642.

Results

SOC in paddy fields and in situ *nitrogen content of phototrophic biofilms*

Before zooming in on the effects of SOC on the community structure and nitrogen immobilization functions of paddy phototrophic biofilms we first established the SOC in paddy fields under study, measured the nitrogen contents of phototrophic biofilms in those fields, and tested the working hypothesis that nitrogen content would increase with increasing SOC. SOC levels in the topsoil varied greatly, from 7.6 to 39.1 g/kg (Fig. 1A), while STN contents were 0.3-6.1 g/kg (Fig. S2). The *in-situ* nitrogen contents of paddy phototrophic biofilms varied from 3.0 (±1.1 S.D.) to 16.0 (±5.1 S.D.) mg TN/g dry biomass (Fig. 1B). From south to northeast (regions I&III, Fig. S1) in China, the biomass nitrogen contents of paddy phototrophic biofilms showed an increasing trend, while from west to east along the Yangtze River (region II), there was a decreasing trend. Despite the regional difference, the biomass nitrogen content had a significant positive correlation with SOC (Fig. 1C, $r = 0.345$, $p < 0.001$), indicating potential effects of SOC on nitrogen immobilization by phototrophic biofilms at SWI in paddy fields.

Characterizing phototrophic biofilm community and N immobilization at varying SOC

Zooming in on the effects of SOC and the labile fractions DOC on the community structure and the nitrogen interception functions of paddy phototrophic biofilms we then set up a controlled microcosm experiment. In this experiment SOC conditions were shown to have distinct effects on the community compositions of phototrophic biofilms. Generally, diversity of both bacteria and algae increased at elevated SOC levels. The cyanobacterial families *Nostocaceae* and *Leptolyngbyaceae* were abundant in all the treatments (Fig. S4A), yet *Nostocaceae* had higher relative abundance in the six treatments than in the control (CK), while the relative abundance of *Leptolyngbyaceae* decreased with increasing SOC and DOC contents. The bacterial family *Alphaproteobacteria*, had significantly positive correlations with DOC ($r = 0.453$, $p < 0.05$) and SOC ($r = 0.557$, $p < 0.01$), while others such as *Chitinophagaceae*, *Planctomycetales*, *Sphingomonadaceae* and *Spirosomaceae* had significant difference between treatments (all $p < 0.05$), but without significant correlations with SOC and DOC (all $p > 0.05$). For algae (Fig. S4B), *Carteria*, *Characiochloris*, *Chlamydomonas* and *Desmodesmus* were abundant genera. DOC and SOC had negative but insignificant correlations with some algae genera including *Desmodesmus*, *Nautococcs*, *Spirosomaceae* and *Chlamydomonas*.

With regards to biofilm biomass and nitrogen contents of that biomass (biomass N), both showed an increasing trend with increasing SOC levels (Fig. S3), with the highest biomass and biomass N observed at the highest initial SOC and DOC contents (i.e. treatment F). Moreover, the biomass N had significantly positive correlations with algal diversity (Fig. 2, $r = 0.673$, $p < 0.01$), bacterial diversity ($r = 0.549$, $p < 0.01$), biomass ($r = 0.813$, $p < 0.01$), DOC content ($r = 0.782$, $p < 0.01$), SOC content ($r = 0.617$, $p < 0.01$), polysaccharide contents ($r = 0.564$, $p < 0.01$), protein contents ($r = 0.548$, $p = 0.011$), and the relative abundance of alga *Uronema* ($r = 0.589$, $p < 0.01$). However, the bacteria family *Leptolyngbyaceae* had significantly negative correlation with biomass N ($r = -0.581$, $p < 0.01$). Similar to biomass N, the biomass (represented by dry weight) had significantly positive correlations with DOC ($r = 0.942$, $p < 0.01$), SOC ($r = 0.856$, $p < 0.01$) and protein content ($r = 0.478$, $p = 0.028$). These positive correlations indicated that SOC was important in driving the growth of phototrophic biofilms. Among the various components in SOC, As the bioactive part, DOC most probably had driven the growth of phototrophic biofilms. Besides, the significantly positive correlation between biomass and algal diversity ($r = 0.695$, $p < 0.01$) suggested

potential impacts of algal diversity on biomass accumulation.

Ecological effects of SOC and DOC on N immobilization by phototrophic biofilms

Considering the high activity and availability of DOC to phototrophic biofilms, two structural equation models (SEM) were set up to assess the effects of both SOC and DOC on the phototrophic community structure, EPS content, biomass accumulation and nitrogen immobilization (Fig. 3). The DOC model (Fig. 3B) had better performance (e.g. lower χ^2 value and higher p value) and explained more of the variance (60.4%) in nitrogen immobilization than the SOC model (56.8%, Fig. 3A). Specifically, the models indicated that both SOC and DOC had strong and positive effects on biomass (path coefficients: 0.827 and 0.78, both $p < 0.001$), bacterial diversity (path coefficients: 0.269 and 0.35, $p = 0.032$ and 0.029 respectively), with the strongest effects on biomass. DOC also had strong effects on polysaccharide contents (path coefficient: 0.249, $p = 0.043$), while SOC had weak effects. Bacteria are pioneers in the formation of phototrophic biofilms with strong and positive effects of bacterial diversity on polysaccharide and algal diversity in the two models. Algae are the main contributors to biomass accumulation in phototrophic biofilms, and here algal diversity had strong and positive effects on biomass (path coefficient: 0.433, $p < 0.001$) and biomass N (path coefficient: 0.197, $p = 0.042$) in the DOC model. However, in the SOC model algal diversity had weak effects on biomass (path coefficient: 0.136, $p > 0.05$). Similar to the significantly positive correlations between biomass and biomass N (Fig. 2), the SEM results verified the strong and positive effects of biomass on nitrogen immobilization in biomass (path coefficients: 0.68 and 0.664, both $p < 0.001$). Polysaccharide, which plays key roles in the initial colonization of phototrophic biofilms, had weak and insignificant effects on algal diversity (path coefficients: 0.054, $p > 0.05$) and biomass nitrogen contents (path coefficients: 0.04, $p > 0.05$) of the mature phototrophic biofilms in the two models. However, polysaccharide had stronger effects on biomass in the SOC model (path coefficient: 0.25, $p < 0.05$) than the DOC model (path coefficient: 0.061, $p > 0.05$). Overall, SOC especially DOC had impacts on biomass accumulation and nitrogen immobilization of phototrophic biofilms via influencing the community.

Metatranscriptomics of phototrophic biofilms along SOC gradients

Differentially expressed genes of phototrophic biofilms from the six treatments compared to the control were annotated with KEGG orthology (KO) allowing the relative expression of KO gene families within a KEGG module to be examined. Proportion of the differentially expressed gene numbers of KEGG modules to the total KEGG annotated gene numbers yielded the rich factor, which highlighted the differences between phototrophic biofilms cultivated under varying SOC and DOC conditions. Overall, the rich factor at low SOC and DOC levels was lower than that at high SOC or DOC levels (Fig. 4). Photosynthesis antenna proteins and photosynthesis were the two KEGG modules for which the different expression increased most under conditions of increased SOC and DOC, and expression of these two pathways peaked at treatment F, representing about 10% and 6% of mapped KEGG genes respectively. In addition, other pathways including ribosome, protein export, carbon fixation in photosynthetic organisms and nitrogen metabolism were also differentially expressed. As indicated by the color in Fig. 4, the rich factors of photosynthesis antenna proteins, photosynthesis and carbon fixation increased with increasing SOC and DOC contents. For instance, the rich factor of photosynthesis antenna proteins increased from 0.061 in treatment A to 0.108 in F. For photosynthesis, the rich factor was 0.043 in treatment A, while it was 0.056 in treatment F. For carbon fixation in photosynthetic organisms, the rich factor increased from 0 in treatment A to 0.024 in F.

Plasticity in the KEGG module expression patterns, especially the expression of photosynthesis and carbon fixation, suggested that SOC or DOC enrichment had elevated growth rate of phototrophic biofilms. This was in accordance with the biofilm biomass observed under varying SOC and DOC conditions (Fig. S3E). Another significantly expressed KEGG module related to growth rate was ribosome, with a rich factor of 2.5-3.4% in A-F, further verifying the increase in biomass accumulation under high SOC and DOC conditions. Besides the growth-related modules, nitrogen metabolism KEGG module was differentially expressed (1.1-2.1%), indicating potential effects of SOC or DOC on nitrogen metabolism of phototrophic biofilms.

To elucidate the effects of SOC and DOC on growth and nitrogen immobilization in more detail, KO gene families related to photosynthesis and nitrogen metabolism were further examined (Figs. 5 and 6). The relative expression of these individual KO gene families varied greatly, but the enzymes related to a pathway exhibited a similar,

apparently coordinated response. For example, the different expressions of enzymes for key processes in PSII (e.g. *PsbA*, *PsbD*, *PsbC* and *PsbB*), PSI (e.g. *PsaA* and *PsaB*), and photosynthesis antenna proteins (e.g. *ApcA*, *ApcE*, *CpcB*, *CpcC* and *CpcG*) all tended to increase as SOC and DOC levels increased (Fig. 5). For nitrogen immobilization, the distinctly expressed KO gene families were mainly *GLT1* and *GLU* in glutamate synthase (Fig. 6), with larger rich factors at high SOC and DOC levels. This affirmed the potent effects of SOC and DOC on inorganic nitrogen immobilization especially the transformation of ammonia to L-Glutamate.

Discussion

Nitrogen immobilization by phototrophic biofilms is a complex process being affected by a mixture of factors including the structure and the physiological status of the community, and the nutrient supply.[22, 41, 42] Here, we answered three questions aimed at elucidating the effects of SOC on nitrogen immobilization by phototrophic biofilms on paddy soils and identifying the pathways behind this immobilization, and thereafter proposing regulating measures for increasing the *in-situ* nitrogen interception by phototrophic biofilms. Based on analyses of phototrophic biofilms collected in paddy fields with different levels of SOC and on microcosm experiments, we present the first empirical evidence that *in-situ* SOC level is central to influencing the community structure, photosynthesis and ultimately inorganic nitrogen immobilization by phototrophic biofilms in paddy fields. Our results show that at high SOC, and especially at high DOC levels, biofilm biomass and nitrogen immobilization were linked with high community diversity and distinct expression of photosynthesis and nitrogen assimilation related gene groups (Figs. 4-6).

Species diversity is key in influencing the functioning of a community or ecosystem, and a common pattern is that biomass production increases with diversity.[43-45] Due to the resource partitioning of nutrients by different species, the species-rich community has higher capacity of completely using different forms of nutrients, with biotic feedbacks on community functions.[14, 15, 46] In this study, our microcosm experiment verified that both biomass production and nitrogen immobilization increased with algal diversity. Algae, the main contributor to biomass yield and nitrogen immobilization in phototrophic biofilms, mainly take up inorganic nitrogen including nitrate and ammonia.[20, 47] However, in soil/sediment more than 90% nitrogen exists in

organic forms, such as amino acid nitrogen, amino sugar nitrogen, hydrolysable unidentified nitrogen and non-hydrolysable nitrogen, which can't be directly assimilated by algae.[48] Mineralization of organic matter by bacteria is the main way through which organic nitrogen is transformed into inorganic nitrogen bioavailable to algae.[49] In other words, the complementarity of species-rich bacteria community must have facilitated the mineralization of organic nitrogen in soil.[50] That should be part of the reason that bacterial diversity had positive effects on algal diversity.

For algae, nitrogen immobilization is an active transport process with a high demand on ATP production, which is related to photosynthesis.[47] In return, the increased uptake of nitrogen by algae prompts algal growth and photosynthesis. Ross et al. [17] reported that high nitrogen uptake by filamentous algae *Cladophora parriaudii* and *Cladophora coelothrix* was followed by high daily growth rate and yielded biomass rich in carbohydrates. Here, we found distinctly different expressions of many KO groups in photosynthesis at high SOC levels (Fig. 5), indicating potent effects of SOC enrichment on triggering photosynthesis. Besides, the KO group of glutamate synthesis was distinctly expressed at high SOC levels (Fig. 6), indicating the effects of SOC on inorganic nitrogen assimilation of phototrophic biofilms. In summary, photosynthesis, biomass accumulation and nitrogen immobilization of phototrophic biofilms are complementary to each other, closely related to SOC levels.

In soil, organic matter is the substrate and energy source for growth of heterotrophic bacteria and nitrogen mineralization.[31, 50] Here bacterial diversity had significant and positive correlations with the SOC and DOC contents (Fig. 2), implying that sufficient SOC supply especially DOC facilitated the formation of species-rich community. In return, species-rich bacterial community releases more inorganic nitrogen into soil via mineralization, with consequent effects on enhancing inorganic nitrogen assimilation by algae. This was consistent with the study of Berthrong et al. [51] that green manure treated soil (SOC enrichment) had higher soil microbial diversity, accumulated more nitrogen in microbial biomass than the control (12.8 vs. 10.5 μg N/g dry soil), and also mineralized twice as much nitrogen as the control (44 vs. 23 μg N/g dry soil). By elucidating the cause-effect relationships among SOC, community structure, photosynthesis, and nitrogen metabolism in the controlled microcosm experiments, we verified the positive correlations between SOC and nitrogen contents

in phototrophic biofilms from paddy fields. Overall, the underlying pathways of SOC enrichment triggering nitrogen interception by phototrophic biofilms at SWI is postulated that: (1) SOC especially DOC enrichment facilitates the formation of species-rich community and prompted photosynthesis; (2) the high diversity induced higher biomass accumulation and nitrogen immobilization; (3) the elevated photosynthesis prompted the synthesis of L-Glutamate and thereby the immobilization of inorganic nitrogen.

Supporting information

Sampling sites location and STN contents in Chinese paddy fields, content changes of DOC, SOC, biomass, biomass N, and EPS, community composition of phototrophic biofilms, and the number of reads mapped to reference of the microcosm experiment.

Declaration of Competing Interest

The authors report no declarations of interest.

Acknowledgements

This work was supported by the National Natural Science Foundation of China (41977101, 41825021), the Natural Science Foundation of Jiangsu Province, China (BK20181511, BE2020731), and Chinese Academy of Sciences.

References

1. Wu, Y.; Liu, J.; Rene, E. R. Periphytic biofilms: A promising nutrient utilization regulator in wetlands. *Bioresour. Technol.* **2018,** *248*, 44-48.

2. Weng, B.; Huang, F.; Zhu, G. B.; Li, H.; Nie, S. A.; Yang, X.; Zhu, Y. G.; Zhang, Z. Nitrogen loss by anaerobic oxidation of ammonium in rice rhizosphere. *ISME J.* **2015,** *9*, 2059-2067.

3. Li, Z.; Liu, Z.; Anderson, W.; Yang, P.; Wu, W.; Tang, H.; You, L. Chinese rice production area adaptations to climate changes, 1949-2010. *Environ. Sci. Technol.* **2015,** *49*, 2032.

4. Lu, H.; Qi, W.; Liu, J.; Bai, Y.; Tang, B.; Shao, H. Paddy periphyton: Potential roles for salt and nutrient management in degraded mudflats from coastal reclamation. *Land Degrad. Dev.* **2018,** *29*, 2932-2941.

5. Yao, Y.; Zhang, M.; Tian, Y.; Zhao, M.; Zhang, B.; Zhao, M.; Zeng, K.; Yin, B. Duckweed (*Spirodela polyrhiza*) as green manure for increasing yield and reducing nitrogen loss in rice production. *Field Crops Res.* **2017,** *214*, 273-282.

6. Voermans, J. J.; Ghisalberti, M.; Ivey, G. N. A Model for mass transport across the sediment-water interface. *Water Resour. Res.* **2018,** *54*, 2799-2812.

7. Thouvenot, M.; Billen, G.; Garnier, J. Modelling nutrient exchange at the sediment–water interface of river systems. *J. Hydrol.* **2007,** *341*, 55-78.

8. Su, J.; Kang, D.; Xiang, W.; Wu, C. Periphyton biofilm development and its role in nutrient cycling in paddy microcosms. *J. Soils Sed.* **2016,** *17*, 810-819.

9. Wu, Y. *Periphyton: functions and application in environmental remediation*. Elsevier: 2016.

10. Liu, J.; Danneels, B.; Vanormelingen, P.; Vyverman, W. Nutrient removal from horticultural wastewater by benthic filamentous algae *Klebsormidium* sp., *Stigeoclonium* spp. and their communities: From laboratory flask to outdoor Algal Turf Scrubber (ATS). *Water Res.* **2016,** *92*, 61-68.

11. Reynaud, P. A.; Roger, P. A. N_2-Fixing Algal Biomass in Senegal Rice Fields. *Ecol. Bull.* **1978**, 148-157.

12. Wu, Y.; Liu, J.; Shen, R.; Fu, B. Mitigation of nonpoint source pollution in rural areas: From control to synergies of multi ecosystem services. *Sci. Total Environ.* **2017,** *607–608*, 1376-1380.

13. Wagg, C.; Bender, S. F.; Widmer, F.; van der Heijden, M. G. A. Soil biodiversity and soil community composition determine ecosystem multifunctionality. *Proc. Natl. Acad. Sci. USA* **2014,** *111*, 5266-5270.

14. Vanelslander, B.; De Wever, A.; Van Oostende, N.; Kaewnuratchadasorn, P.; Vanormelingen, P.; Hendrickx, F.; Sabbe, K.; Vyverman, W. Complementarity effects drive positive diversity effects on biomass production in experimental benthic diatom biofilms. *J. Ecol.* **2009,** *97*, 1075-1082.

15. Barry, K. E.; Mommer, L.; van Ruijven, J.; Wirth, C.; Wright, A. J.; Bai, Y.; Connolly, J.; De Deyn, G. B.; de Kroon, H.; Isbell, F.; Milcu, A.; Roscher, C.; Scherer-Lorenzen, M.; Schmid, B.; Weigelt, A. The future of complementarity: Disentangling causes from consequences. *Trends Ecol. Evol.* **2019,** *34*, 167-180.

16. Liu, J.; Vyverman, W. Differences in nutrient uptake capacity of the benthic filamentous algae *Cladophora* sp., *Klebsormidium* sp. and *Pseudanabaena* sp. under varying N/P conditions. *Bioresour. Technol.* **2015,** *179*, 234-242.

17. Ross, M. E.; Davis, K.; McColl, R.; Stanley, M. S.; Day, J. G.; Semião, A. J. C. Nitrogen uptake by the macro-algae Cladophora coelothrix and Cladophora parriaudii: Influence on growth, nitrogen preference and biochemical composition. *Algal Res.* **2018,** *30*, 1-10.

18. Bracken, M. E. S.; Stachowicz, J. J. Seaweed diversity enhances nitrogen uptake

via complementary use of nitrate and ammonium. *Ecology* **2006,** *87*, 2397-2403.

19. Lu, H.; Feng, Y.; Wang, J.; Wu, Y.; Shao, H.; Yang, L. Responses of periphyton morphology, structure, and function to extreme nutrient loading. *Environ. Pollut.* **2016,** *214*, 878-884.

20. Liu, J.; Wu, Y.; Wu, C.; Muylaert, K.; Vyverman, W.; Yu, H. Q.; Munoz, R.; Rittmann, B. Advanced nutrient removal from surface water by a consortium of attached microalgae and bacteria: A review. *Bioresour. Technol.* **2017,** *241*, 1127-1137.

21. Boelee, N. C.; Temmink, H.; Janssen, M.; Buisman, C. J. N.; Wijffels, R. H. Nitrogen and phosphorus removal from municipal wastewater effluent using microalgal biofilms. *Water Res.* **2011,** *45*, 5925-5933.

22. Bharti, A.; Velmourougane, K.; Prasanna, R. Phototrophic biofilms: diversity, ecology and applications. *J. Appl. Phycol.* **2017,** *29*, 2729-2744.

23. Schmidt, M. W. I.; Torn, M. S.; Abiven, S.; Dittmar, T.; Guggenberger, G.; Janssens, I. A.; Kleber, M.; Kögel-Knabner, I.; Lehmann, J.; Manning, D. A. C.; Nannipieri, P.; Rasse, D. P.; Weiner, S.; Trumbore, S. E. Persistence of soil organic matter as an ecosystem property. *Nature* **2011,** *478*, 49.

24. Tiessen, H.; Cuevas, E.; Chacon, P. The role of soil organic matter in sustaining soil fertility. *Nature* **1994,** *371*, 783-785.

25. Neumann, D.; Heuer, A.; Hemkemeyer, M.; Martens, R.; Tebbe, C. C. Importance of soil organic matter for the diversity of microorganisms involved in the degradation of organic pollutants. *ISME J.* **2014,** *8*, 1289.

26. Flemming, H.-C.; Wingender, J. The biofilm matrix. *Nat. Rev. Microbiol.* **2010,** *8*, 623-633.

27. Roeselers, G.; Van Loosdrecht, M.; Muyzer, G. Heterotrophic pioneers facilitate phototrophic biofilm development. *Microb. Ecol.* **2007,** *54*, 578-585.

28. Miqueleto, A.; Dolosic, C.; Pozzi, E.; Foresti, E.; Zaiat, M. Influence of carbon sources and C/N ratio on EPS production in anaerobic sequencing batch biofilm reactors for wastewater treatment. *Bioresour. Technol.* **2010,** *101*, 1324-1330.

29. Lee, J.; Park, J. H.; Shin, Y. S.; Lee, B. C.; Chang, N. I.; Cho, J.; Kim, S. D. Effect of dissolved organic matter on the growth of algae, Pseudokirchneriella subcapitata, in Korean lakes: The importance of complexation reactions. *Ecotoxicol. Environ. Saf.* **2009,** *72*, 335-343.

30. Li, D.; Sharp, J. O.; Saikaly, P. E.; Ali, S.; Alidina, M.; Alarawi, M. S.; Keller, S.; Hoppe-Jones, C.; Drewes, J. E. Dissolved organic carbon influences microbial community composition and diversity in managed aquifer recharge systems. *Appl. Environ. Microbiol.* **2012,** *78*, 6819-6828.

31. Zhang, W.; Xu, M.; Wang, X.; Huang, Q.; Nie, J.; Li, Z.; Li, S.; Hwang, S. W.; Lee, K. B. Effects of organic amendments on soil carbon sequestration in paddy fields of subtropical China. *J. Soils Sed.* **2012,** *12*, 457-470.

525 32. Lam, T. Y. C.; Mei, R.; Wu, Z.; Lee, P. K. H.; Liu, W.-T.; Lee, P.-H. Superior
526 resolution characterisation of microbial diversity in anaerobic digesters using full-
527 length 16S rRNA gene amplicon sequencing. *Water Res.* **2020,** *178*, 115815.

528 33. Shakya, M.; Lo, C. C.; Chain, P. S. G. Advances and challenges in
529 metatranscriptomic analysis. *Front. Genet.* **2019,** *10*, 904.

530 34. Mei, F.; Wu, X.; Yao, C.; Li, L.; Wang, L.; Chen, Q. Rice cropping regionalization
531 in China. *Chinese J. of Rice Sci.* **1988,** *2*, 97-110.

532 35. Liu, J.; Tang, J.; Wan, J.; Wu, C.; Graham, B.; Kerr, P. G.; Wu, Y. Functional
533 sustainability of periphytic biofilms in organic matter and Cu^{2+} removal during
534 prolonged exposure to TiO_2 nanoparticles. *J. Hazard. Mater.* **2019,** *370*, 4-12.

535 36. Panova, M.; Aronsson, H.; Cameron, R. A.; Dahl, P.; Godhe, A.; Lind, U.; Ortega-
536 Martinez, O.; Pereyra, R.; Tesson, S. V. M.; Wrange, A.-L.; Blomberg, A.; Johannesson,
537 K. DNA extraction protocols for whole-genome sequencing in marine organisms. In
538 *Marine Genomics: Methods and Protocols*, Bourlat, S. J., Ed. Springer New York: New
539 York, NY, 2016; pp 13-44.

540 37. Callahan, B. J.; Wong, J.; Heiner, C.; Oh, S.; Theriot, C. M.; Gulati, A. S.; McGill,
541 S. K.; Dougherty, M. K. High-throughput amplicon sequencing of the full-length 16S
542 rRNA gene with single-nucleotide resolution. *Nucleic Acids Res.* **2019,** *47*, e103.

543 38. Dixon, P. VEGAN, a package of R functions for community ecology. *J Veg. Sci.*
544 **2003,** *14*, 927-930.

545 39. Revelle, W. R. psych: Procedures for personality and psychological research.
546 *Software* **2017**.

547 40. Rosseel, Y. lavaan: An R Package for Structural Equation Modeling. *J Stat. Softw.*
548 **2012,** *48*, 1-36.

549 41. Larned, S. T. A prospectus for periphyton: recent and future ecological research. *J.*
550 *N. Am. Benthol. Soc.* **2010,** *29*, 182-206.

551 42. Li, J.; Deng, K.; Hesterberg, D.; Xia, Y.; Wu, C.; Xu, R. Mechanisms of enhanced
552 inorganic phosphorus accumulation by periphyton in paddy fields as affected by
553 calcium and ferrous ions. *Sci. Total Environ.* **2017,** *609*, 466-475.

554 43. Weis, J. J.; Cardinale, B. J.; Forshay, K. J.; Ives, A. R. Effects of species diversity
555 on community biomass production change over the course of succession. *Ecology* **2007,**
556 *88*, 929-939.

557 44. Power, L. D.; Cardinale, B. J. Species richness enhances both algal biomass and
558 rates of oxygen production in aquatic microcosms. *Oikos* **2010,** *118*, 1703-1711.

559 45. van Ruijven, J.; Berendse, F. Diversity–productivity relationships: Initial effects,
560 long-term patterns, and underlying mechanisms. *Proc. Natl. Acad. Sci. USA* **2005,** *102*,
561 695-700.

562 46. García, F. C.; Bestion, E.; Warfield, R.; Yvon-Durocher, G. Changes in

563 temperature alter the relationship between biodiversity and ecosystem functioning.
564 *Proc. Natl. Acad. Sci. USA* **2018,** *115*, 10989-10999.

565 47. Cai, T.; Park, S. Y.; Li, Y. Nutrient recovery from wastewater streams by
566 microalgae: Status and prospects. *Renew. Sust. Energ. Rev.* **2013,** *19*, 360-369.

567 48. Inselsbacher, E. Recovery of individual soil nitrogen forms after sieving and
568 extraction. *Soil Biol. Biochem.* **2014,** *71*, 76-86.

569 49. Bengtsson, G.; Bengtson, P.; Månsson, K. F. Gross nitrogen mineralization-,
570 immobilization-, and nitrification rates as a function of soil C/N ratio and microbial
571 activity. *Soil Biol. Biochem.* **2003,** *35*, 143-154.

572 50. Bongoua-Devisme, A. J.; Cebron, A.; Kassin, K. E.; Yoro, G. R.; Mustin, C.;
573 Berthelin, J. Microbial communities involved in Fe reduction and mobility during soil
574 organic matter (SOM) mineralization in two contrasted paddy soils. *Geomicrobiol. J.*
575 **2013,** *30*, 347-361.

576 51. Berthrong, S. T.; Buckley, D. H.; Drinkwater, L. E. Agricultural management and
577 labile carbon additions affect soil microbial community structure and interact with
578 carbon and nitrogen cycling. *Microb. Ecol.* **2013,** *66*, 158-170.

Figure legend

Fig. 1 The box plots of total organic carbon content in soil (SOC, %, A) and total nitrogen contents in paddy phototrophic biofilms biomass (biomass N, % of dry weight, B), C: Correlationship between SOC and nitrogen immobilization capacity of paddy phototrophic biofilms (i.e. biomass N contents) from the 20 sampling sites over China (n = 200, I: South China, II: the middle and lower reaches of Yangtze River, III: Northeast China).

Fig. 2 Correlation heatmap of SOC, DOC and phototrophic biofilm community characteristics including abundant genera and families, diversity, biomass, EPS components and nitrogen contents in biomass in the microcosm experiment. Different color intensities represent Spearman correlation coefficients. Significant correlations are indicated with asterisks: * $p < 0.05$, ** $p < 0.01$, *** $p < 0.001$.

Fig. 3 The effects of (A) soil organic carbon (SOC) and (B) dissolved organic carbon (DOC) on nitrogen immobilization in phototrophic biofilms using the structural equation model (SEM). The red line represents the significantly effect, and grey line represents insignificant effect. The width of arrows indicates the strength of the causal effects. R^2 represents the proportion of variance explained for each variable. For SOC, $\chi^2 = 5.820$, $p = 0.221$, df = 3, GFI = 0.988, RMSEA = 0.112. For DOC, $\chi^2 = 0.894$, $p = 0.925$, df = 4, GFI = 0.998, RMSEA = 0.000. Numbers above arrows indicates the standard path coefficient. * $p < 0.05$; ** $p < 0.01$; *** $p < 0.001$. Bacteria: bacterial diversity; Algae: algal diversity.

Fig. 4 The enriched KO groups for phototrophic biofilms under varying SOC conditions (Treatments A-F vs. CK). Color indicates the proportion of differentially expressed gene numbers of each KEGG module to the total annotated gene numbers at that KEGG module.

Fig. 5 Schematic model depicting the different expression of KO gene families associated with photosynthesis pathways for phototrophic biofilms under varying SOC conditions (Treatments A-F vs. CK). Color indicates the proportion of differentially expressed gene numbers of each KEGG module relative to the total annotated gene numbers at that KEGG module.

Fig. 6 Schematic model depicting the different expression of KO gene families associated with nitrogen metabolism pathways including nitrate reduction, denitrification, nitrogen fixation, nitrification, and Glutamate synthesis for phototrophic biofilms under varying SOC conditions (Treatments A-F vs. CK). Color indicates the proportion of differentially expressed gene numbers of each KEGG module relative to the total annotated gene numbers at that KEGG module.

Figures

Fig. 1

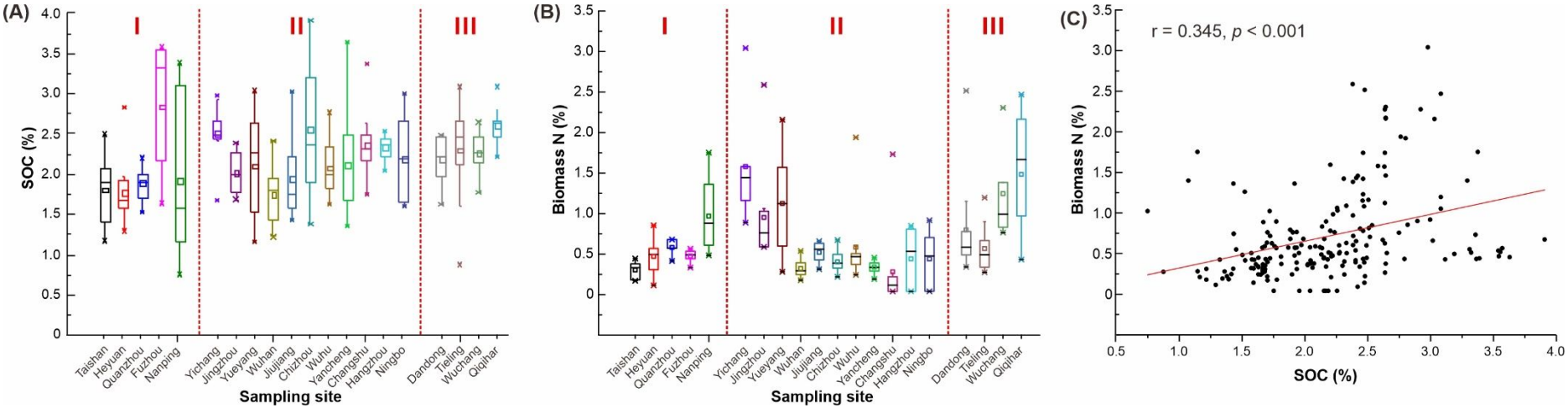

619 **Fig. 2**

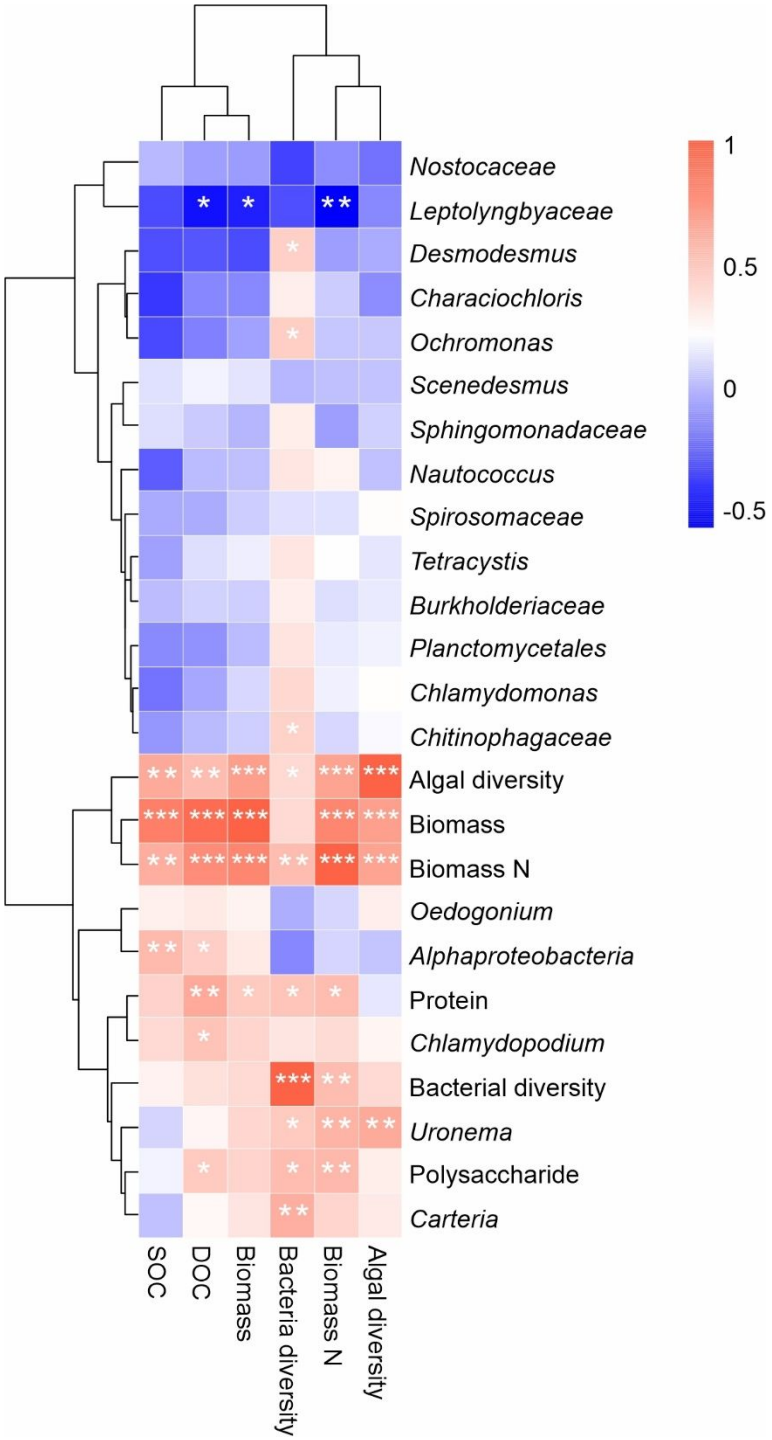
Nostocaceae
Leptolyngbyaceae
Desmodesmus
Characiochloris
Ochromonas
Scenedesmus
Sphingomonadaceae
Nautococcus
Spirosomaceae
Tetracystis
Burkholderiaceae
Planctomycetales
Chlamydomonas
Chitinophagaceae
Algal diversity
Biomass
Biomass N
Oedogonium
Alphaproteobacteria
Protein
Chlamydopodium
Bacterial diversity
Uronema
Polysaccharide
Carteria
SOC
DOC
Biomass
Bacteria diversity
Biomass N
Algal diversity
1
0.5
0
-0.5

620

621 **Fig. 3**

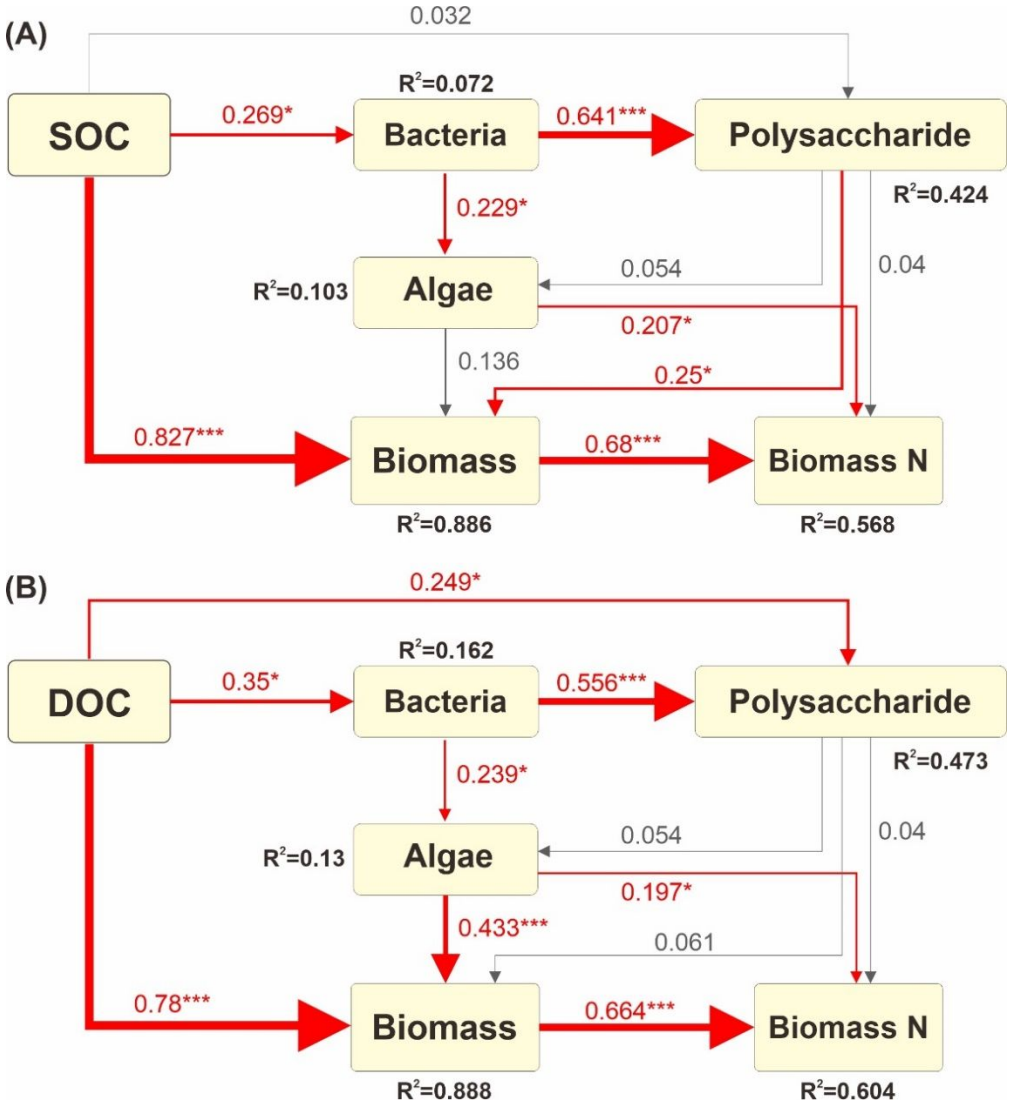
(A)
0.032
SOC
0.269*
R²=0.072
Bacteria
0.641***
Polysaccharide
R²=0.424
0.229*
0.04
R²=0.103
Algae
0.054
0.207*
0.136
0.25*
0.827***
Biomass
0.68***
Biomass N
R²=0.886
R²=0.568
(B)
0.249*
DOC
0.35*
R²=0.162
Bacteria
0.556***
Polysaccharide
R²=0.473
0.239*
0.04
R²=0.13
Algae
0.054
0.197*
0.433***
0.061
0.78***
Biomass
0.664***
Biomass N
R²=0.888
R²=0.604

622

623 **Fig. 4**

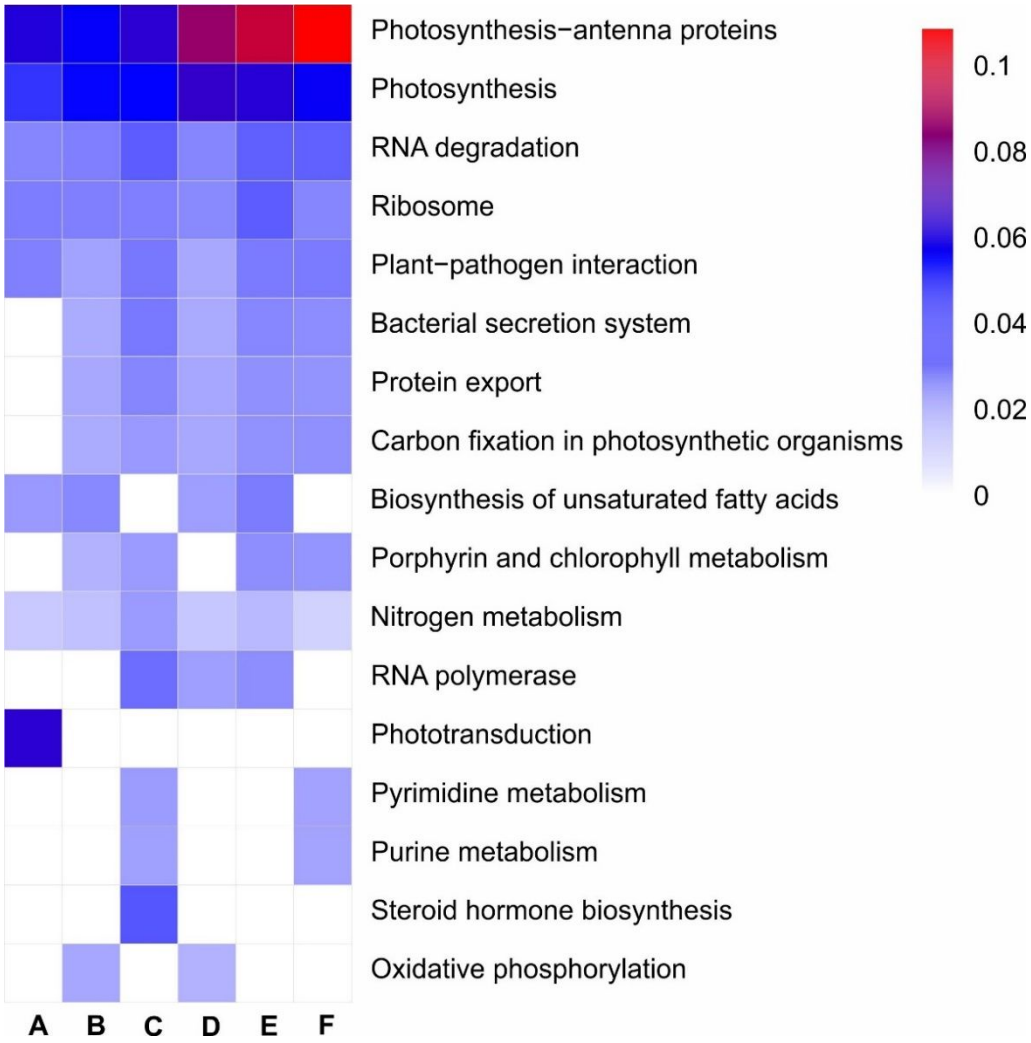
Photosynthesis−antenna proteins
Photosynthesis
RNA degradation
Ribosome
Plant−pathogen interaction
Bacterial secretion system
Protein export
Carbon fixation in photosynthetic organisms
Biosynthesis of unsaturated fatty acids
Porphyrin and chlorophyll metabolism
Nitrogen metabolism
RNA polymerase
Phototransduction
Pyrimidine metabolism
Purine metabolism
Steroid hormone biosynthesis
Oxidative phosphorylation
A B C D E F
0.1
0.08
0.06
0.04
0.02
0

624

625 **Fig. 5**

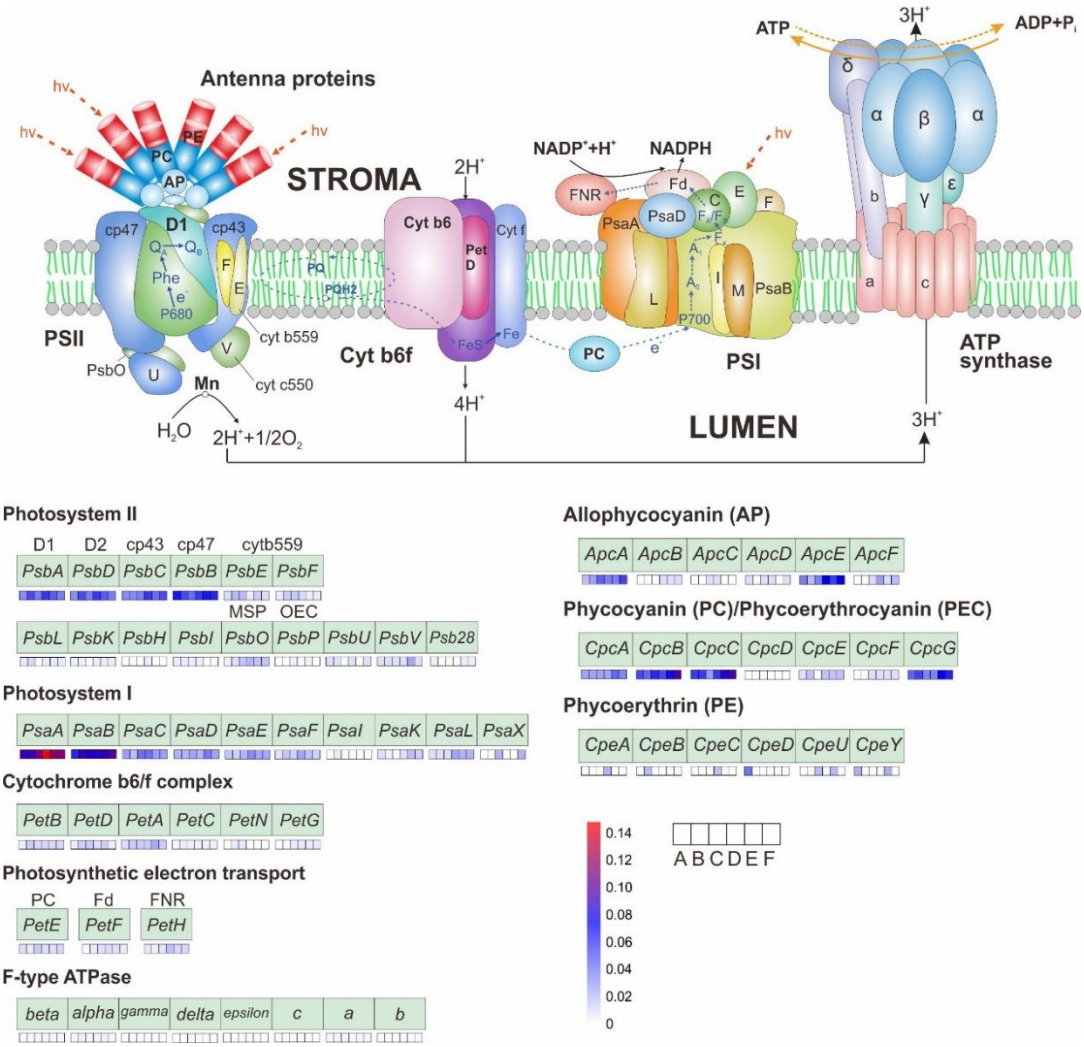

Photosystem II

D1	D2	cp43	cp47	cytb559					
PsbA	*PsbD*	*PsbC*	*PsbB*	*PsbE*	*PsbF*				
				MSP	OEC				
PsbL	*PsbK*	*PsbH*	*PsbI*	*PsbO*	*PsbP*	*PsbU*	*PsbV*	*Psb28*	

Photosystem I

PsaA	*PsaB*	*PsaC*	*PsaD*	*PsaE*	*PsaF*	*PsaI*	*PsaK*	*PsaL*	*PsaX*

Cytochrome b6/f complex

PetB	*PetD*	*PetA*	*PetC*	*PetN*	*PetG*

Photosynthetic electron transport

PC	Fd	FNR
PetE	*PetF*	*PetH*

F-type ATPase

beta	*alpha*	*gamma*	*delta*	*epsilon*	*c*	*a*	*b*

Allophycocyanin (AP)

ApcA	*ApcB*	*ApcC*	*ApcD*	*ApcE*	*ApcF*

Phycocyanin (PC)/Phycoerythrocyanin (PEC)

CpcA	*CpcB*	*CpcC*	*CpcD*	*CpcE*	*CpcF*	*CpcG*

Phycoerythrin (PE)

CpeA	*CpeB*	*CpeC*	*CpeD*	*CpeU*	*CpeY*

626

627 **Fig. 6**

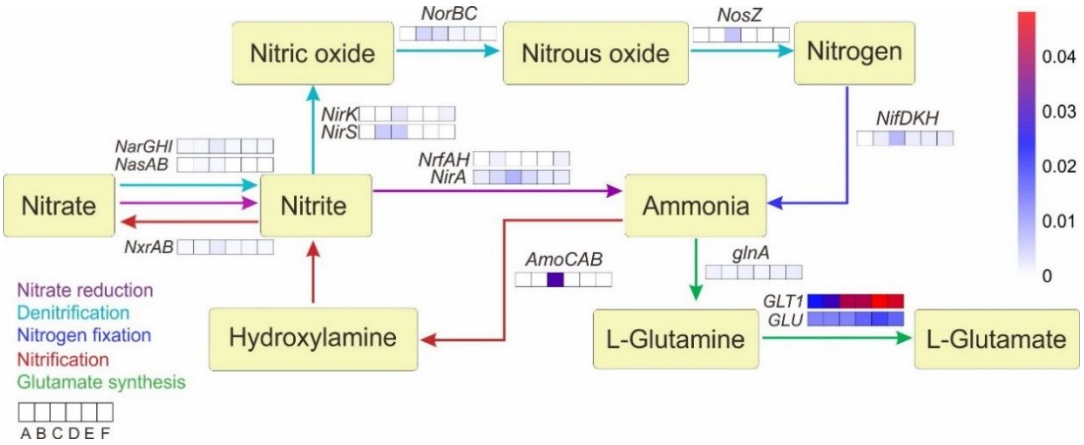
Nitric oxide
Nitrous oxide
Nitrogen
NorBC
NosZ
NirK
NirS
NifDKH
NarGHI
NasAB
NrfAH
NirA
Nitrate
Nitrite
Ammonia
NxrAB
AmoCAB
glnA
GLT1
GLU
Hydroxylamine
L-Glutamine
L-Glutamate
0.04
0.03
0.02
0.01
0
Nitrate reduction
Denitrification
Nitrogen fixation
Nitrification
Glutamate synthesis
A B C D E F

628